# A MULTI-DEGREE-OF-FREEDOM ELECTROSTATIC MEMS POWER HARVESTER

**Zi Jing Wong, Jize Yan, Kenichi Soga, and Ashwin A. Seshia**
Department of Engineering, University of Cambridge, UK

**Abstract:** This paper reports the design, modeling and experimental characterization of a multi-degree-of-freedom electrostatic vibration energy harvester. The potential of harvesting vibrational energy at multiple input frequencies and achieving displacement amplification in the response is investigated. To better understand the device performance at a system level, a numerical model which incorporates mechanical and electrical analysis in a charge constrained conversion circuit is developed. Experimental results on a microfabricated prototype demonstrate a maximum measured output power of 0.076 μW at 1.4 kHz for an external load of 5.1 MΩ. We also experimentally demonstrate that the output power varies with the square of input acceleration and DC bias voltage.

**Keywords:** electrostatics, MEMS, energy harvesting, multi-degree-of-freedom

## INTRODUCTION

Piezoelectric, electromagnetic and electrostatic transducers integrated into vibratory structures allow for the harvesting and conversion of ambient vibrational energy into an electrical form [1]. There is great interest in the design and realization of MEMS scale vibrational energy harvesters and in their application to the integration and powering of autonomous MEMS sensor nodes. As compared to piezoelectric and electromagnetic transduction, the electrostatic power harvester (EPH) is readily realized through conventional microfabrication technology. However, the EPH trails other transduction schemes in terms of power generation capability [2].

Most previous research focused on optimizing a single-degree-of-freedom (SDOF) vibratory structure to harvest the vibration energy at a particular frequency [1-2]. In reality, however, ambient vibration in large-scale civil and mechanical structures usually possesses a broadband frequency spectrum with multiple resonant frequencies. In addition, the resonant frequencies may shift considerably over the operating lifetime and due to environmental variations.

To overcome the above problems, we propose a multi-degree-of-freedom electrostatic power harvester (MDOF EPH) that is designed to display more than a single resonance frequency in the vibration spectrum of interest. In addition, we propose the applicability of this principle to amplify the vibration-induced displacement as compared to the case for a SDOF EPH. Analytical modeling and experimental tests are performed to characterize the device performance.

## PRINCIPLE OF OPERATION

The idea of a MDOF EPH is inspired in part by the Stockbridge damper which is a vibration absorber used to reduce the vibration amplitude of power lines at resonance. Conceptually, in a system with a smaller mass attached to a bigger mass, the displacement of the bigger mass can be transferred to the smaller mass while being amplified. This happens at a specific frequency which depends strongly on the choice of system parameters. Further, a *n*-degree-of-freedom (*n*DOF) system would lead to *n* resonant peaks in the frequency response that can be tuned based on the application.

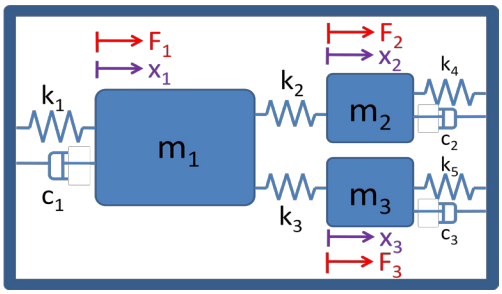


*Fig. 1: A 3DOF spring-mass-damper system.*

Fig. 1 shows a 3DOF mechanical spring-mass-damper model. The comparison is to the case of a SDOF system comprising a large mass of value equal to the summation of $m_1$, $m_2$ and $m_3$. The 3DOF system is generated by dividing the large mass into three smaller masses, and two inner springs $k_2$ and $k_3$ are introduced to mechanically connect between the masses. $c_1$, $c_2$, and $c_3$ are damping coefficients dominated by the squeeze film damping between moving and fixed electrodes. The governing equations for the 3DOF EPH are given by

$$[M]\ddot{X} + [C]\dot{X} + [K]X = F \quad (1)$$

where

$$[M] = \begin{bmatrix} m_1 & 0 & 0 \\ 0 & m_2 & 0 \\ 0 & 0 & m_3 \end{bmatrix} \quad [C] = \begin{bmatrix} c_1 & 0 & 0 \\ 0 & c_2 & 0 \\ 0 & 0 & c_3 \end{bmatrix}$$

$$[K] = \begin{bmatrix} k_1 + k_2 + k_3 & -k_2 & -k_3 \\ -k_2 & k_2 + k_4 & 0 \\ -k_3 & 0 & k_3 + k_5 \end{bmatrix}$$

$$F = \begin{Bmatrix} F_1 \\ F_2 \\ F_3 \end{Bmatrix} = \begin{Bmatrix} m_1\ddot{y} \\ -m_2\ddot{y} \\ m_3\ddot{y} \end{Bmatrix}$$

$F$ is the force vector which denotes the inertia force acting on each mass due to the external acceleration $\ddot{y}$. The displacement, velocity and acceleration are represented by vectors $X$, $\dot{X}$ and $\ddot{X}$.

A 3DOF system with $m$, $k$ and $c$ values as shown in Fig. 2(a) would produce a forced response consisting of three resonant peaks. By designing the peaks close to each other, a quasi-broadband effect is realized wherein a larger induced displacement is obtained within a certain specified frequency band. This is particularly relevant for a MEMS EPH which operates in air, and is susceptible to high squeeze-film damping. Fig. 2(b) demonstrates the possibility of shifting the resonant frequencies by changing the stiffness of the inner springs $k_2$ and $k_3$. This is essential to match to the frequency response of the vibration source or to attain a quasi-broadband response of a certain bandwidth. Fig. 2(c) is an illustration of how the displacement amplitude of the first mode of a symmetrical system could be amplified (by 117% in this case) by simply changing the direction of the applied force on $m_2$. This, however, comes at the expense of suppressing the second vibration mode. Compared to a SDOF case, with a combined mass, $m$ of 0.8 µkg (i.e. $m_1+m_2+m_3$), $k$ of 70 N/m (i.e. $k_1+k_4+k_5$), and $c$ of 300 µNs/m (i.e. $c_1+c_2+c_3$), the maximum displacement amplitude observed for this MDOF system is still 3.5% higher. Further displacement amplification could be obtained by careful design of the mass and stiffness parameters.

## SYSTEM-LEVEL MODEL

To understand the performance of the designed MDOF EPH at both the device and circuit levels, an electromechanically coupled numerical model is developed. The Matlab Simulink model is based on the charge-constrained operating condition and the general computation flow is shown in Fig. 3. It is essentially an extension of the model developed in [3] and [4-5]. The important features include:

- Combine a 3DOF spring-mass-damper system with electrostatic force feedback;
- Allow direct input of time-domain non-sinusoidal and random input acceleration;
- Detect contact and pull-in instability;
- Implement circuit with switch control and threshold setting to simulate how charges accumulate, decay and transfer to the load.

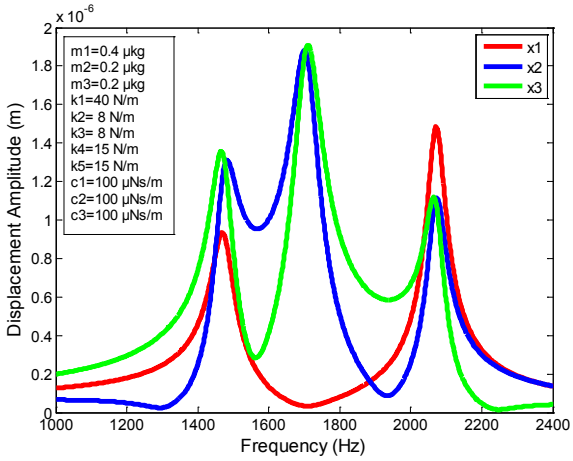


(a)

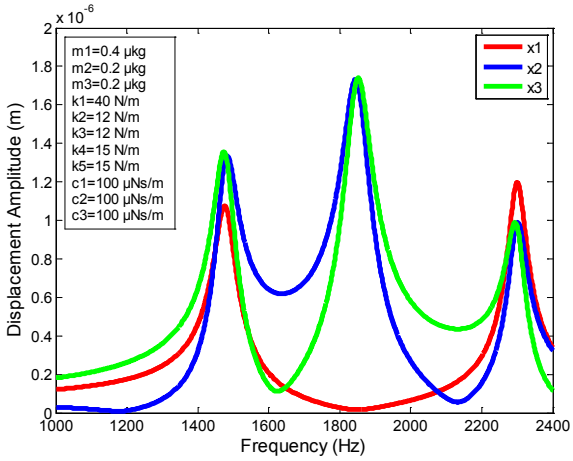


(b)

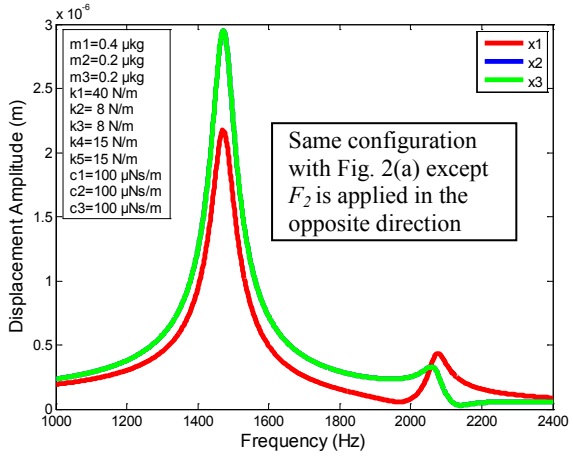


(c)

*Fig. 2: Forced response of 3DOF system with different design parameters.*

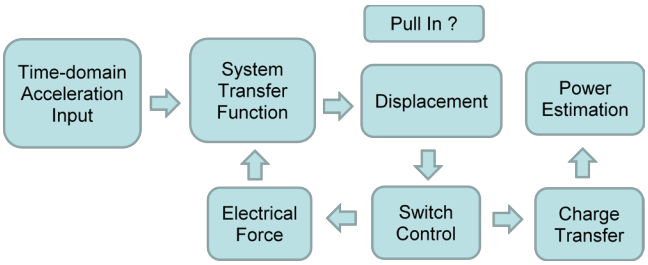


*Fig. 3: Flow of the numerical system-level model.*

*Table 1: Parameters used in numerical model*

| Parameter | Symbol | Value |
|---|---|---|
| Width of electrode fingers | $w_f$ | 10 µm |
| Length of electrode fingers | $l_f$ | 400 µm |
| Overlap length of electrode fingers | $L_f$ | 390 µm |
| Gap spacing between electrode fingers | $g_f$ | 5 µm |
| Number of electrode fingers on $m_1$ | $N_1$ | 146 |
| Number of electrode fingers on $m_2$ | $N_2$ | 80 |
| Number of electrode fingers on $m_3$ | $N_3$ | 80 |
| Amplitude of sinusoidal input acceleration | $a$ | 25 $ms^{-2}$ |
| DC bias voltage | $V_{in}$ | 0.8 V |
| Storage capacitor | $C_{storage}$ | 4 nF |
| Displacement threshold to turn on switch | $x_{th}$ | 3 µm |
| Load resistance | $R_{load}$ | 30 MΩ |

*Table 2: Mass and spring used in numerical model*

| $m_1$ | $m_2$ | $m_3$ | $k_1$ | $k_2$ | $k_3$ | $k_4$ | $k_5$ |
|---|---|---|---|---|---|---|---|
| 0.3565 µkg | 0.1887 µkg | 0.1887 µkg | 40 N/m | 7.3 N/m | 7.3 N/m | 14.26 N/m | 14.26 N/m |

For the case shown in Fig. 2(c), and design parameters as shown in Table 1 and 2, with the assumption of $c$ on each mass of 10 µNs/m, the voltage delivered to the load $V_{out}$ is estimated to reach a steady state level of 0.54 V and 0.45 V, corresponding to a power output $P_{out}$ of 0.0097 µW and 0.00675 µW, for sinusoidal input acceleration at 1506 Hz and 2123 Hz respectively.

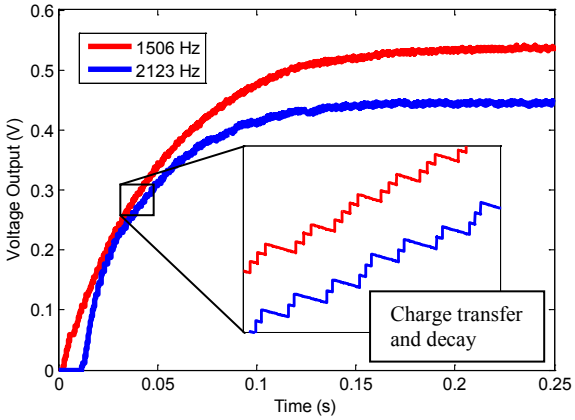


*Fig. 4: Simulated output voltage at load resistor.*

## FABRICATION

The 3DOF EPH is fabricated using the standard SOI-MUMPS foundry process followed by wire bonding and deposition of a self-assembled monolayer (SAM) of Perfluorotrichlorosilane to prevent stiction on contact between moving and fixed electrodes.

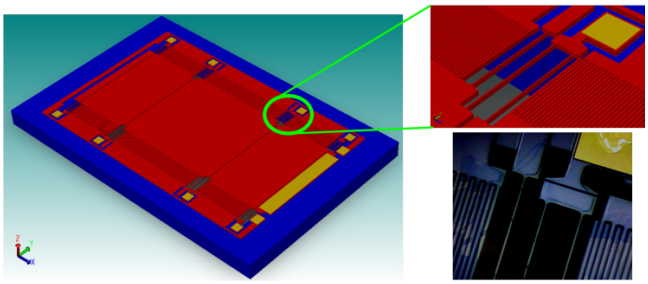

*Fig. 5: 3DOF EPH showing the suspension and electrodes in both schematic and optical micrograph.*

## EXPERIMENTAL

For simplicity, the voltage (and hence power) measurement is carried out in constant voltage mode using an operational amplifier set in a voltage follower configuration, as shown in Fig. 6. The AC current produced is assumed to pass through the load, and thus the power is determined by the square of $V_{out}$ divided by $R_{load}$. A printed circuit board (PCB) was fabricated to integrate electrical components with the MDOF EPH. Most of the tests are performed in air, except for those shown in Fig. 11 which are carried out inside a vacuum chamber. The test setup is shown in Fig. 7 and Fig. 8.

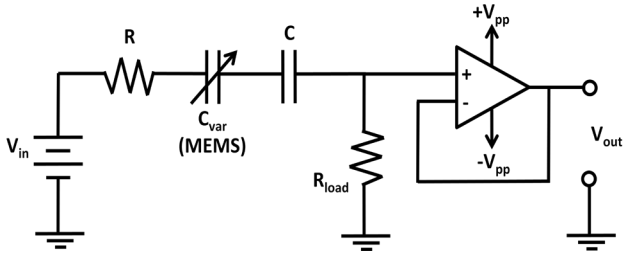


*Fig. 6: Electrical measurement circuit.*

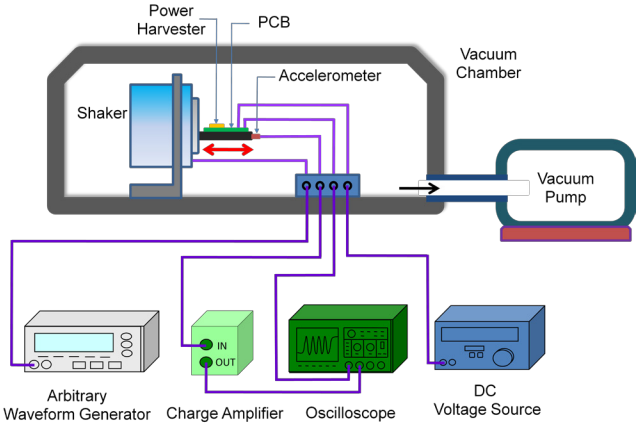


*Fig. 7: Illustration of measurement setup.*

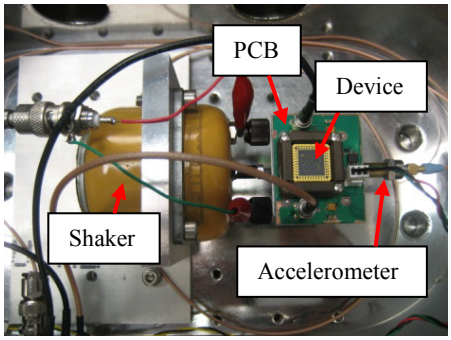


*Fig. 8: A photograph of the test setup in a custom vacuum chamber.*

A series of tests are performed to characterize the device performance in terms of its maximum power output, and the influence of input acceleration magnitude, DC bias voltage and pressure on output power. The input frequency coincides with the resonance of the first vibration mode.

The maximum measured peak-to-peak voltage $V_{out\ p\text{-}p}$ is 0.88 V at 1.4 kHz for an $R_{load}$ of 5.1 MΩ at an input acceleration of 1.53 $ms^{-2}$. This corresponds to a $P_{out}$ of approximately 0.076 µW. The other results are shown in Figs. 9-11. It can be seen that $P_{out}$ varies with the square of input acceleration and bias voltage. The reduction of $P_{out}$ above 4 V is due to the EPH reaching pull-in instability. The result in Fig. 11 suggests that $P_{out}$ behaves in a similar manner to the quality factor $Q$, increasing substantially beyond a certain pressure threshold. The higher $Q$ allows for larger vibration amplitude and thus higher $P_{out}$.

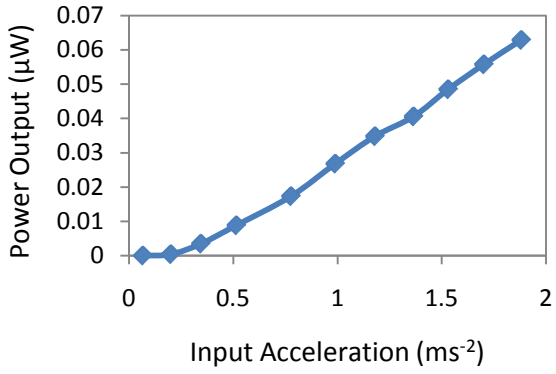


*Fig. 9: Plot of output power versus input acceleration.*

## CONCLUSION

The design principles, system-level modeling and characterization of a three-degree-of-freedom electrostatic MEMS power harvester are presented. A multi-degree-of-freedom EPH has the potential advantage of displacement amplification and harnessing external vibrations over a broader frequency spectrum. The maximum measured power output for a fabricated prototype is 0.076 µW at 1.4 kHz for an external load of 5.1 MΩ.

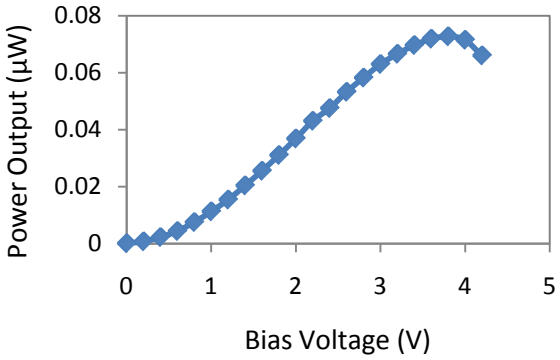


*Fig. 10: Effect of DC bias voltage on output power.*

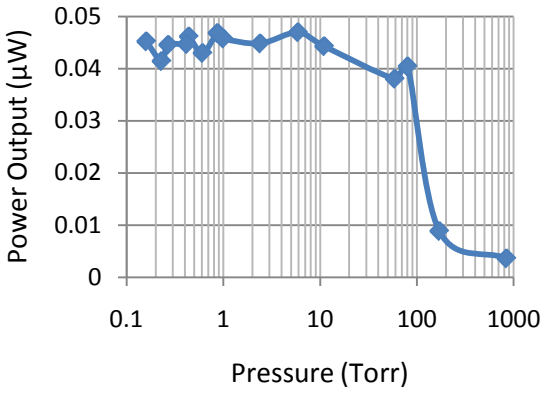


*Fig. 11: Effect of pressure on output power.*

## REFERENCES

[1] Beeby S P, Tudor M J, White N M 2006 Energy harvesting vibration sources for microsystems applications *Meas. Sci. Technol.* **17** R175-R195

[2] Mitcheson P D, Yeatman E M, Rao G K, Holmes, A S, Green T C 2008 Energy harvesting from human and machine motion for wireless electronic devices *Proc IEEE* **96** 1457-1486

[3] Roundy S J 2003 Energy scavenging for wireless sensor nodes with a focus on vibration to electricity conversion *PhD Thesis* University of California Berkeley

[4] Chiu Y, Kuo C T, Chu Y S 2007 MEMS design and fabrication of an electrostatic vibration-to-electricity energy converter *Microsyst. Technol.* **13** 1663-1669

[5] Chiu Y, Tseng V F G 2008 A capacitive vibration-to-electricity energy converter with integrated mechanical switches *J. Micromech. Microeng.* **18** 104004